Probe Report

Title: An inhibitor of the Cdc2-like kinase 4 (Clk4)

Authors: Andrew S. Rosenthal[a], Cordelle Tanega[a], Min Shen[a], Bryan T. Mott[a], James M. Bougie[a], Dac-Trung Nguyen[a], Tom Misteli[b], Douglas S. Auld[a], David J. Maloney[a], Craig J. Thomas[a*]

[a]NIH Chemical Genomics Center, National Human Genome Research Institute, NIH 9800 Medical Center Drive, MSC 3370 Bethesda, MD 20892-3370 USA. [b]Cell Biology of Genomes, National Cancer Institute, NIH, 41 Library Drive, Bethesda, MD 20892 USA.

Version #: 4

Date Submitted: 3/3/2011

Assigned Assay Grant #: R03 MH084827

Screening Center Name & PI: NIH Chemical Genomics Center & Dr. Christopher P.Austin

Chemistry Center Name & PI: NIH Chemical Genomics Center & Dr. Christopher P. Austin

Assay Submitter & Institution: Dr. Tom Misteli, NCI, NIH

PubChem Summary Bioassay Identifier (AID): 1997

Abstract:

The Cdc2-like kinases (Clk's) and the dual-specificity tyrosine phosphorylation-regulated kinases (Dyrk's) have specified roles in gene splicing. Specifically, the Clk class of enzymes has been shown to phosphorylate the SR proteins, which are a major component of the spliceosome. Dyrk1A has been shown to accumulate in nuclear speckles, where it interacts and activates splicing factors. It has been hypothesized that inhibition of these targets may offer a mechanism to control splicing. This probe represents our continued examination of substituted 6-arylquinazolin-4-amines as Clk/Dyrk inhibitors. Several of the most potent inhibitors, including ML167 (CID_44968231) were validated as being highly selective within a comprehensive kinome scan. Appropriate aqueous solubility and stability were found for this agent.

Probe Structure & Characteristics:

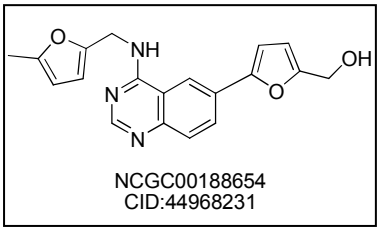

ML#167

CID/ML#	Target Name	IC_{50}/EC_{50} (nM) [SID, AID]	Anti-target Name(s)	IC_{50}/EC_{50} (μM) [SID, AID]	Fold Selective	Secondary Assay(s) Name: IC_{50}/EC_{50} (nM) [SID, AID]
44968231/ ML167	Cdc2-like kinase 4 (Clk4)	136nM [90944997, 2710]	Clk1, Clk2, Clk3, Dyrk1A/1B	> 1μM [90944997, 2710]	>10 fold	Kinase panel [90944997, 2710]

Recommendations for scientific use of the probe:

Kinases are a major target for pharmacological intervention, and kinase inhibitors (both specific and promiscuous) represent important probes and drugs. Small molecule probes that target specific kinases represent critical tools for exploring and controlling cell function. The Cdc2-like kinases (Clk's) and the dual-specificity tyrosine phosphorylation-regulated kinases (Dyrk's) are two classes of enzymes that have been shown to phosphorylate specific proteins within the spliceosome; therefore, they are considered important targets for the modulation of gene splicing events. In addition to the agents reported in these reports, there is only one other reported Clk4 inhibitor, which was found to be somewhat promiscuous versus a kinase panel. Small molecule inhibitors of all 4 isoforms of the Clk family and both the Dyrk1A and Dyrk1B family, with varying selectivity profiles, will be of great utility to the study of these kinases as modulators of gene splicing, as well as other cellular events. The probe described here represents the first fully selective inhibitor of Cdc2-like kinase 4 (Clk4). This probe compound will be useful for the scientific community in unraveling the phenotype associated solely with Clk4 down-regulation without complication arising from the inhibition of related kinases. Particularly,

given the reported role of the Clk family as a specific modulator of SR proteins, this probe will be useful in exploring the specific functions of Clk4 in terms of gene splicing.

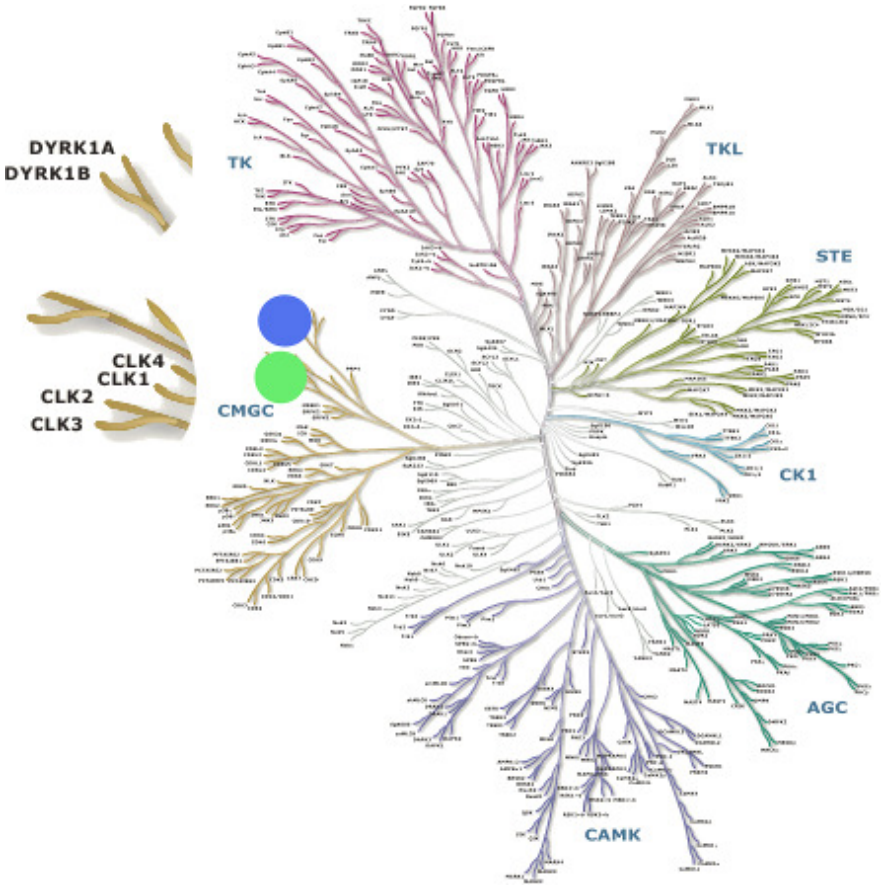

1. Introduction

The removal of intron sequences from genes occurs via the actions of the spliceosome, a protein complex that removes intervening sequences at the nuclear pre-mRNA level to afford properly coded mRNA for translation[1,2]. Many genes produce multiple mRNA isoforms through the actions of alternative splicing and importantly, numerous human diseases are caused by improper splicing[3]. Exogenous manipulation of the spliceosome is theorized to be a powerful means to controlling gene translation and ultimately correct disease phenotypes via rectification of splicing abnormalities. There are several reports of kinases that alter the function of the spliceosome. Among these are the Cdc2-like kinase (Clk) family[4]. A major target of Clk kinases is the prominent family of serine- and arginine-rich (SR) splicing proteins[5,6], which are involved in the assembly of the spliceosome and are implicated in both constitutive and alternative splicing control and selection of splicing sites[7,8]. The Clk family contains four characterized isoforms (Clk1, Clk2, Clk3 and Clk4). The Clks are capable of auto-phosphorylation (at serine, threonine and tyrosine residues) and phosphorylation of exogenous proteins (at serine and threonine residues). Members of the Clk family have been implicated in the regulation of alternative splicing of PKCβII, TF, Tau and β-globin pre-mRNA. These studies suggest that small molecule modulation of the Clk family of kinases may represent an important mechanism for the control of mRNA splicing.

Hagiwara and coworkers have reported TG003 (**1**) (Figure 1) as a small molecule with low-nanomolar IC_{50} values versus Clk1 and Clk4[9]. The report does not define the selectivity of TG003 beyond the Clk family and 4 additional kinases (PKA, PKC, SRPK1 and SRPK2). We have recently reported on NCGC00010037 (CID_3232621; SID_85239684) (**2**), a quinazoline-based ATP-competitive inhibitor of the Clk1, Clk4 and Dyrk1A that retains good potency and selectivity across a panel of 402 kinases (Figure 1). Mott *et al* recently detailed the selectivity of TG003 versus the same 402 kinase panel and revealed that TG003 had several activities, including 19nM, 95nM and 30nM versus Clk1, Clk2 and Clk4, respectively with several

additional activities (CSNK1D (150nM), CSNK1E (300nM), Dyrk1A (12nM), Dyrk1B (130nM), PIM1 (130nM), PIM3 (280nM) and Ysk4 (290nM))[10]. The patent literature revealed structurally similar benzothiazole **1a** from Sirtris Pharmaceuticals[11] and a substituted quinoline from Chronogen, Inc.[12] reported to have activity versus Clk1 (Figure 1). Indole **KH-CB19** was recently revealed as a potent (20nM) ATP competitive Clk1 inhibitor with good selectivity over Clk3 via a unique binding mode[13].

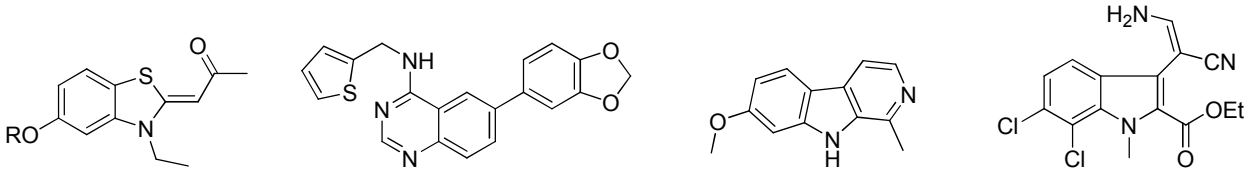

1, R = CH_3 (TG003)
1a, R = H

2 (NCGC00010037)

Harmine

KH-CB19

Based upon the potency and selectivity for **2,** we next aimed to understand the binding mechanism of this chemotype at Clk1 and Clk4. We explored the binding modality by examining the inhibitory capacity of **2** in settings that varied both compound and substrate concentrations. The dose response curve of **2** in the presence of three different ATP concentrations demonstrated a loss in potency when ATP levels rose. Conversely, the % activity of **1** in the presence of varying concentrations of the peptide substrate had no affect on the compound potency. This data strongly suggests that this agent is an ATP-competitive inhibitor of Clk1 and Clk4.

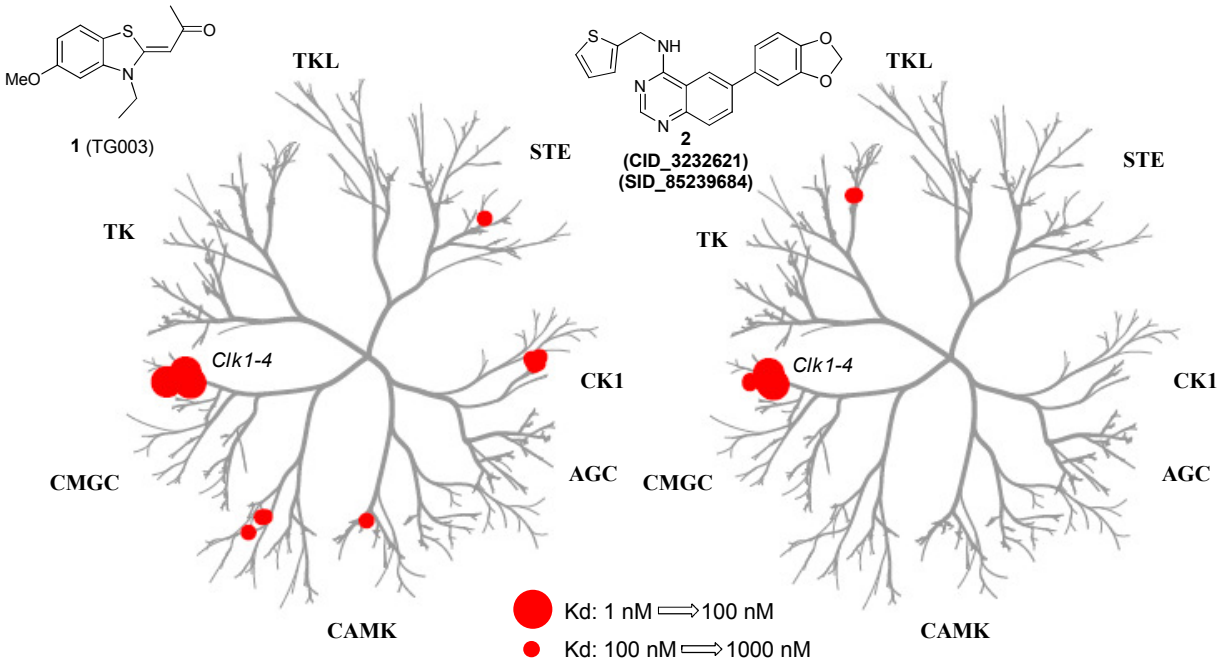

Figure 1. Dendrogram representation of the selectivity profile for kinase binding by TG003 (**1**) and **2** within a panel of 402 kinases.

Activity for **1**: Clk1 = 19nM, Clk2 = 95nM, Clk3 = 3000nM, Clk4 = 30nM, CSNK1D = 150nM, CSNK1E = 300nM, CSNK1G2 = 270nM, CSNK1G3 = 290nM, Dyrk1A = 12nM, Dyrk1B = 130nM, PIM1 = 130nM, PIM3 = 280nM, Ysk4 = 290nM.

Activity for **2**: Clk1 = 37nM, Clk2 = 680nM, Clk3 = 470nM, Clk4 = 50nM, Dyrk1A = 27nM, Dyrk1B = 430nM, EGFR = 230nM.
*Note: **2** was active (>250nM) versus numerous EGFR mutants.*

The ability to ascribe a phenotype to the specific, pharmacological down-regulation of a target is a key aspect of understanding the role of various cellular targets within cellular pathways and events. Small molecule inhibitors that are promiscuous are of limited use, given the complexities associated with understanding their overall cellular response in the context of a single target. Even small molecules that inhibit a reasonable number of cellular targets (< 10) can be plagued by a lack of certainty in terms of phenotype association to a single target. As such, we endeavored to further optimize NCGC00010037 (CID:3232621) (**2**) for specific inhibition of Clk4.

2 Materials and Methods

General Methods for Chemistry: All air or moisture sensitive reactions were performed under positive pressure of nitrogen with oven-dried glassware. Anhydrous solvents such as dichloromethane, *N,N*-dimethylforamide (DMF), acetonitrile, methanol and triethylamine were obtained by purchasing from Sigma-Aldrich. Preparative purification was performed on a Waters semi-preparative HPLC. The column used was a Phenomenex Luna C18 (5 micron, 30x 75mm) at a flow rate of 45 ml/min. The mobile phase consisted of acetonitrile and water (each containing 0.1% trifluoroacetic acid). A gradient of 10% to 50% acetonitrile over 8 minutes was used during the purification. Fraction collection was triggered by UV detection (220nM). Analytical analysis was performed on an Agilent LC/MS (Agilent Technologies, Santa Clara, CA).

Method 1: A 7 minute gradient of 4% to 100% Acetonitrile (containing 0.025% trifluoroacetic acid) in water (containing 0.05% trifluoroacetic acid) was used with an 8 minute run time at a flow rate of 1 ml/min. A Phenomenex Luna C18 column (3 micron, 3x 75mm) was used at a temperature of 50°C.

Method 2: A 3 minute gradient of 4% to 100% Acetonitrile (containing 0.025% trifluoroacetic acid) in water (containing 0.05% trifluoroacetic acid) was used with a 4.5 minute run time at a flow rate of 1 ml/min. A Phenomenex Gemini Phenyl column (3 micron, 3x 100mm) was used at a temperature of 50°C.

Purity determination was performed using an Agilent Diode Array Detector on both Method 1 and Method 2. Mass determination was performed using an Agilent 6130 mass spectrometer with electrospray ionization in the positive mode. ^{1}H NMR spectra were recorded on Varian 400 MHz spectrometers. Chemical Shifts are reported in ppm with tetramethylsilane (TMS) as internal standard (0 ppm) for $CDCl_3$ solutions or undeuterated solvent (DMSO-h6 at 2.49 ppm) for DMSO-d6 solutions. All of the analogs for assay have purity greater than 95% based on both analytical methods. **High resolution mass** spectrometry was recorded on an Agilent 6210 Time-of-Flight LC/MS system. Confirmation of molecular formula was accomplished using

electrospray ionization in the positive mode with the Agilent Masshunter software (version B.02).

2.1 Assays

The application of bioluminescence to ATPases assay has relied on a substrate depletion format. In these assays, the ATP dependence of firefly luciferase is used to measure the remaining ATP concentration, where the luminescence signal is inversely proportional to kinase activity[14-17]. To provide a signal-to-background of approximately 2-fold, the substrate must be depleted by at least 50%. Operating enzyme assays under these high conversion conditions is not at all optimal for classical enzymological studies. However, this is acceptable for HTS, as shifts in potency are typically less than 2-fold with a percent conversion < 80%. Given that HTS assays typically show variability in potency determinations between ~2-3-fold, shifts due to high conversions in the range of 50-80%, will not be easily discernable from the assay noise even if the assay is performed at lower conversions. Therefore, ATP-depletion has become a popular choice to perform generic HTS assays for ATPases, particularly protein kinases.

We used two bioluminescent assays for the Clk4 assay (Figure 2). Measurement of ATP depletion was assessed by using the Kinase-Glo™ assay system, where a firefly luciferase detection reagent containing D-luciferin and buffer components are added to detect the remaining ATP, following the Clk4 kinase assay (Figure 2A). The second system, ADP-Glo® measures kinase activity by quantifying the amount of ADP formed after the kinase reaction. Bioluminescent detection of ADP levels is achieved through the addition two different detection reagents (Figure 2B). First, a reagent that stops the protein kinase reaction and depletes the remaining ATP is added. Then, a second reagent is added to stop ATP degradation. In addition, the second reagent also contains an enzyme, such as pyruvate kinase, that efficiently converts the ADP to ATP and the same firefly luciferase/D-luciferin components present in Kinase-Glo, which generate the luminescent signal proportional to the ADP concentration produced. Therefore, the two assay formats show opposite luminescent signal changes in response to protein kinase inhibitors.

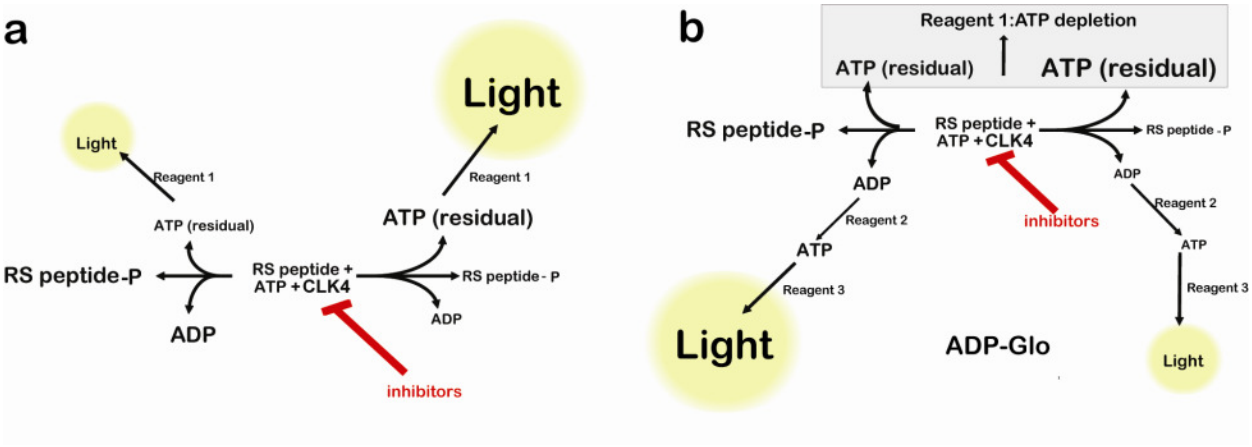

Figure 2. Bioluminescent assays used for Clk4 qHTS. **A**. Bioluminescent measurement of ATP depletion using Kinase-Glo. **B**. Bioluminescent measurement of ADP formation using ADP-Glo.

All compounds were screened using a qHTS approach[14], where compounds are assayed using at least seven concentrations to generate concentration-response curves for every compounds. The methodology for creating a concentration-titration series between successive copies of library plates for the purpose of large-scale titration-based screening has been described. Briefly, qHTS uses an inter-plate dilution method where the first plate contains the highest concentration of a set of compounds in DMSO, while subsequent plates contain the same compounds in the same well locations, but at successive lower concentrations. Using the protocol outlined above, we calculated a plate throughput of 18 plates/hr, or approximately 7 samples/sec, on the Kalypsys robotic system, which means that a 7 point CRC was obtained every second on the robotic system.

Table 1. Assay protocol: The optimized 1536-well protocol.

	Kinase-Glo			ADP-Glo		
Step	**Parameter**	**Value**	**Description**	**Parameter**	**Value**	**Description**
1	Reagent	2µl	ATP/peptide	Reagent	2µl	ATP/peptide
2	Library	23nl	0.5 nM- 46 µM	Library	23nl	0.6 nM- 55.2 µM
3	Controls	23nl	TG003	Controls	23nl	TG003
4	Reagent	1µl	Clk4	Reagent	0.5µl	Clk4
5	Time	4.5 hrs	r.t. incubation	Time	1 hr	r.t. incubation
6	Reagent	3µl	Kinase-Glo	Reagent	2.5µl	Deplete ATP
7	Read	2 sec	ViewLux	Time	45 min	r.t. incubation
8				Reagent	5µl	ADP→ATP/Luc
9				Time	30 min	r.t. incubation
10				Read	2 sec	ViewLux
Step	Notes			Notes		
1	100µM RS peptide, 1µM ATP (final) concentration in buffer; FRD dispense			100µM RS peptide, 1µM ATP (final) concentration in buffer; FRD dispense		
2	Pin-tool transfer compound library for a (final) range of 46µM to 0.5nM			Pin-tool transfer compound library for a (final) range of 55.2µM to 0.6nM		
3						
4	Clk4 at 25nM final, FRD dispense			Clk4 at 25nM final, FRD dispense		

The assay showed excellent performance (the signal-to-background ratio was 3.2 +/- 0.07, the average Z' screening factor associated with each plate was 0.86 +/- 0.02 and the CV was 7.2 +/- 1.9, indicating a robust performance of the screen).

Additional assays were performed by commercial vendors, including Reaction Biology (www.reactionbiology.com) and Ambit Biosciences (www.ambitbio.com). Reaction Biology relies upon a ^{33}P-γ-ATP radiometric based filtration binding assay, and the Ambit assay is based upon a competition binding assay of kinases fused to a proprietary tag.

2.2 Probe Chemical Characterization

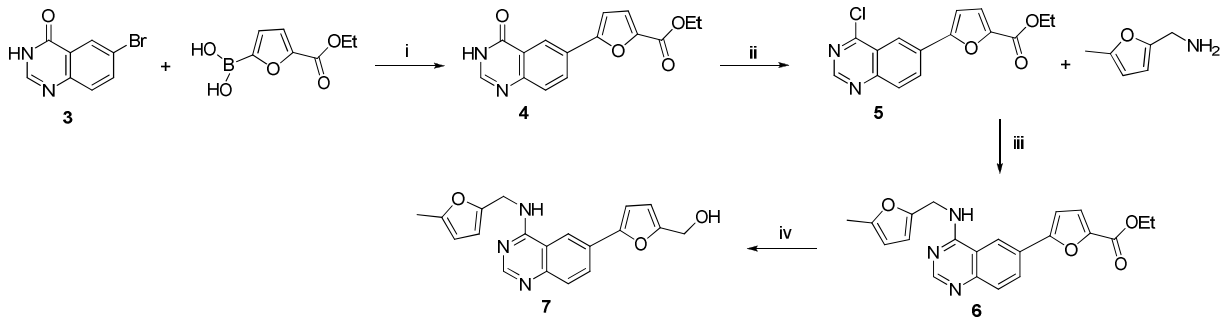

Scheme 1. Reagents and conditions: (i) $Pd(PPh_3)_4$, Na_2CO_3, DME, H_2O, 150 ºC (MW), 1.5 h (typical yields: 40-50%); (**ii**) $POCl_3$, N,N-dimethylaniline, toluene, reflux, 1 h; (iii) DIPEA, DMF, rt, 2 h (typical yields: 80-95%); (iv) LAH, THF, rt, 15 min (typical yields: 80-95%).

NCGC00188654/CID:44968231/ML167: 1H NMR (400 MHz, DMSO-d6) δ 8.79 - 8.93 (2 H, m), 8.69 - 8.79 (1 H, m), 8.22 - 8.36 (1 H, m), 7.75 - 7.91 (1 H, m), 6.99 - 7.16 (1 H, m), 6.48 - 6.60 (1 H, m), 6.26 - 6.38 (1 H, m), 6.01 - 6.12 (1 H, m), 4.88 (2 H, br. s.), 4.51 (2 H, br. s.), 2.24 (3 H, br. s.). LC/MS: Method 1, retention time: 2.865 min; Method 2, retention time: 3.917 min. HRMS: m/z (M+H) = 336.1343 (Calculated for C19H18N3O3 336.1348). Solubility (PBS, pH 7.4, 23°C) = 20.1µM. Stability profile over 48 hrs (PBS, pH 7.4, 23°C) is shown below.

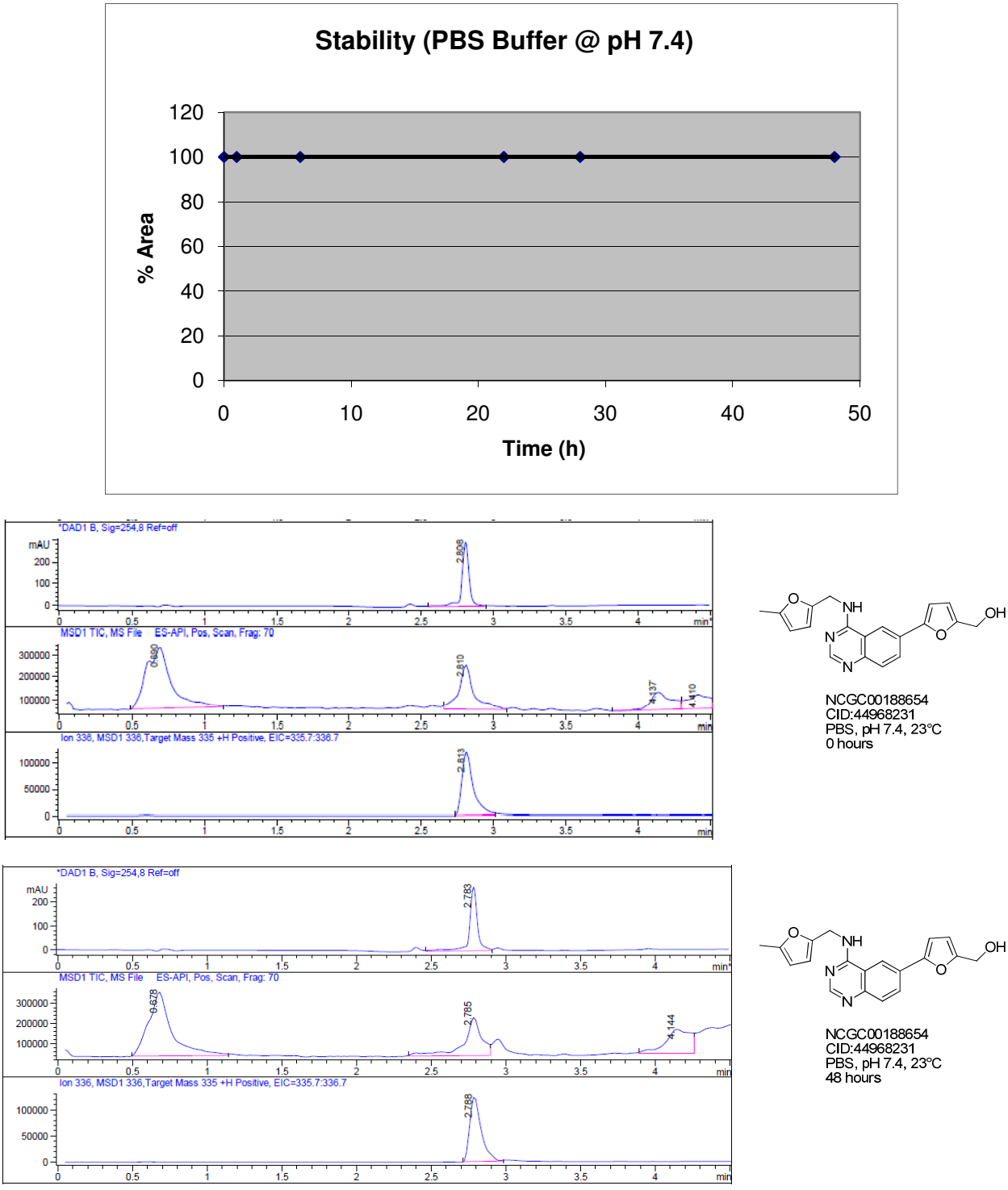

Figure 3. LCMS traces of NCGC00188654/CID:44968231/ML167 in PBS buffer, pH 7.4 at 23°C at 0 hours and 48 hours.

MLS Numbers for Probe and Analogs:

NCGC ID	MLS ID
NCGC00188654-01	MLS002729079 (Probe)
NCGC00185966-01	MLS003179280
NCGC00185976-01	MLS003179275
NCGC00185985-01	MLS003179269
NCGC00189261-01	MLS003179268
NCGC00229611-01	MLS003179266

2.3 Probe Preparation

The production of *N*-substituted-6-arylquinazolin-4-amines can be accomplished via two similar synthetic approaches. The synthesis of NCGC00010037 (CID:3232621) (**2**) was accomplished via the addition of thiophen-2-ylmethanamine to 6-bromo-4-chloroquinazoline in DMF with Hunig's base at room temperature. The resulting product was then subjected to standard Suzuki-Miyaura couplings with benzo[d][1,3]dioxol-5-ylboronic acid using tetrakis(triphenylphosphine)palladium(0) and sodium carbonate in DMF and heating using microwave irradiation. This general procedure resulted in the production of numerous *N*-substituted-6-arylquinazolin-4-amines. Alternatively, the synthesis of NCGC00188654 (CID:44968231) began with the Suzuki-Miyaura coupling of 6-bromoquinazolin-4(3H)-one (**3**) to 5-(ethoxycarbonyl)furan-2-ylboronic acid. The resulting ethyl 5-(4-oxo-3,4-dihydroquinazolin-6-yl)furan-2-carboxylate (**4**) was treated with $POCl_3$ to derive ethyl 5-(4-chloroquinazolin-6-yl)furan-2-carboxylate (**5**). Addition of (5-methylfuran-2-yl)methanamine in basic DMF displaced the chlorine to arrive at ethyl 5-(4-((5-methylfuran-2-yl)methylamino)quinazolin-6-yl)furan-2-carboxylate (**6**), and a standard LAH reduction of the ethyl ester provided the probe compound (5-(4-((5-methylfuran-2-yl)methylamino)quinazolin-6-yl)furan-2-yl)methanol (NCGC00188654, CID:44968231)(**7**) in good overall yield.

3 Results

The identification of these agents as potent inhibitors of Clk1, Clk4, Dyrk1A and Dyrk1B was discovered following their assessment in a cell-based assay aimed at identifying modulators of Lamin A splicing. As the assay description (found in PubChem) describes:

"Hutchinson-Gilford Progeria Syndrome (HGPS) is a pediatric premature aging disease caused by a spontaneous mutation in the lamin A/C (LMNA) gene. The mutation activates a cryptic splice site in the LMNA pre-mRNA which results in production of a pre-lamin A protein that cannot be processed properly. The mutant protein accumulates in the nucleus and negatively affects numerous cellular functions. Correction of the splicing defect in HGPS patient cells using a targeted oligonucleotide (exo11) leads to reversal of the cellular disease phenotypes. To identify small molecule modulators of aberrant LMNA splicing, a homogenous assay was constructed in HeLa cells that used a GFP containing minigene to report on correction of aberrant splicing in lamin A and a RFP (DsRed2) to report on cell viability, uniformity and nonspecific effects on the assay signal."

The discovery of quinoline-based agents as putative actives in this screen strongly suggested kinase activity as a mechanism by which the splicing correction was being manifested. A literature search uncovered the Cdc2-like kinase (Clk) family as a modifier of the prominent family of serine- and arginine-rich (SR) splicing proteins. Examination of the lead compounds in a Clk4 assay found that these agents were indeed capable of potent inhibition of the target. Following this realization, we aimed to optimize this compound class for potent and selective inhibition of the Clk class of kinases. During a selectivity examination of several of these compounds, we discovered that these compounds were further capable of inhibiting the Dyrk class of kinases, which are also implicated in splicing modulation via the phosphorylation of the splicing factor SF3b1. At the present time, agents have been discovered with activity at Clk4, Clk1, Dyrk1A and Dyrk1B (with varying degrees of selectivity). These agents represent the largest collection of Clk and Dyrk inhibitors, and several boast the best reported potency for these targets. The mechanism of action strongly suggests that these are ATP-competitive kinase inhibitors, which is in alignment with other known quinazoline-based kinases inhibitors, and molecular dynamic simulations and modeling support this assessment. Several cell-based assays are now being examined to establish these compounds (and the role of their targets) in broader

phenotypical outcomes, including the role of the Clk and Dyrk kinases as modulators of gene splicing.

3.1 Summary of Screening Results

Not applicable (the activity at Clk4 and related kinases was uncovered from leads found in the qHTS Assay for Modulators of Lamin A Splicing; AID 1487).

Identification of lead

This screening effort revealed several small molecule Clk4 inhibitors within the high confidence 1a, 1b and 2c concentration-response curves (CRCs; class 1 curves display two asymptotes, an inflection point, and $r^2 \geq 0.9$; subclasses 1a and 1b are differentiated by full (>80%) vs. partial (≤ 80%) response, respectively, while class 2a curves display a single left-hand asymptote and inflection point and full (>80%) response)[17]. A cheminformatics analysis of the qHTS data included chemotype clustering, singleton identification, analysis of orthogonal activities, and structural considerations, which included physical properties and anticipated optimization potential. Potency range and maximum response was additionally considered. Ultimately, this analysis led us to focus on the substituted quinazoline NCGC00010947 (CID:3233528) (**8**) (Figure 4). Our first rounds of synthesis and evaluation identified NCGC00010037 (CID:3232621) (**9**) as a potent Clk1, Clk4 and Dyrk1A inhibitor.

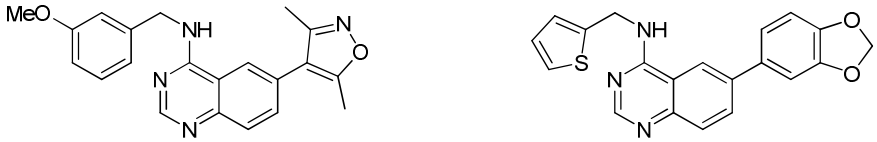

8 (NCGC00010947)
CID:3233528

9 (NCGC00010037)
CID:3232621

Figure 4. Structure of NCGC00010947 (**8**) and NCGC00010037 (**9**).

3.2 Dose Response Curves for Probe

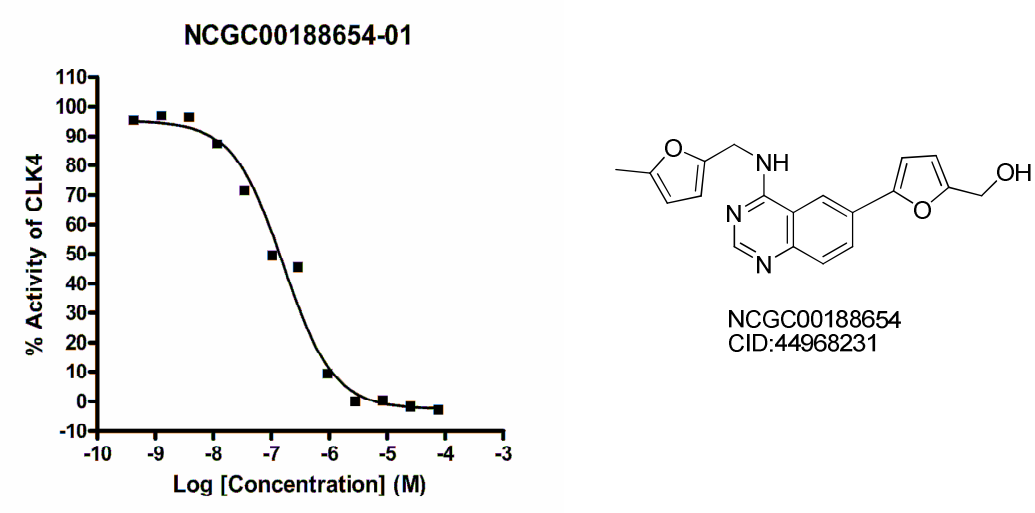

Figure 5. Structure of NCGC00188654/CID:44968231/ML167 and dose response curve for in-house Clk4 assay.

3.3 Scaffold/Moiety Chemical Liabilities

NCGC00188654/CID:44968231/ML167 contains a furan ring which may be liable to *in vivo* metabolism.

3.4 SAR Tables

Table 2. Inhibition at Clk1-4 and Dyrk1A and Dyrk1B for selected quinazoline based Clk4 inhibitors

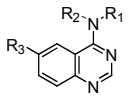

							Target		Antitargets			
Entry	NCGCID	SID	CID	R_1	R_2	R_3	Clk4 IC_{50} (nM)	Clk1 IC_{50} (nM)	Clk2 IC_{50} (nM)	Clk3 IC_{50} (nM)	Dyrk1A IC_{50} (nM)	Dyrk1B IC_{50} (nM)
2	00010037	85239684	3232621	**H**			**39**	**59**	**1902**	**6936**	**62**	**697**
7 (Probe)	00188654	90944997	44968231	**H**		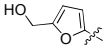	**136**	**1522**	**1648**	**> 10000**	**> 10000**	**4420**
10	00012272	85239693	3234850	**H**			**249**	**915**	**714**	**> 10000**	**1262**	**405**
11	00188642	90944985	44968219	**H**			**490**	**2820**	**5049**	**> 10000**	**3388**	**2872**
12	00188644	90944987	44968221	**H**		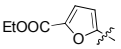	**229**	**2083**	**6181**	**> 10000**	**3629**	**7990**
13	00188647	90944990	44968224	**Me**			**269**	**899**	**1209**	**> 10000**	**1136**	**304**
14	00188648	90944991	44968225	**Me**		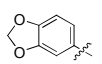	**120**	**480**	**3331**	**> 10000**	**922**	**4036**
15	00188650	90944993	44968227	**Me**		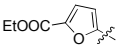	**239**	**916**	**7203**	**> 10000**	**1501**	**3867**
16	00188653	90944996	44968230	**Me**	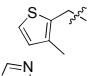	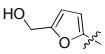	**81**	**206**	**889**	**> 10000**	**557**	**352**
17	00188673	90945016	44968250	**H**	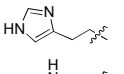	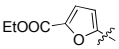	**254**	**1054**	**7280**	**> 10000**	**1406**	**2401**
18	00188681	90945024	44968258	**H**		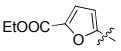	**790**	**6644**	**> 10000**	**> 10000**	**2706**	**5534**
19	00188686	90945029	44968263	**H**	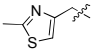		**340**	**2379**	**3132**	**> 10000**	**4820**	**1889**
20	00185981	85239768	44223970	**Me**	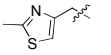	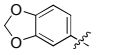	**11**	**20**	**186**	**1924**	**14**	**25**
21	00188682	90945025	44968259	**H**	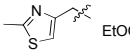	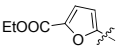	**813**	**6266**	**ND**	**ND**	**8307**	**>10000**
22	00185963	85239750	44223952	**H**	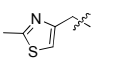	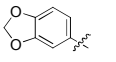	**40**	**96**	**1327**	**7448**	**206**	**1510**
23	00229610	99380785	46916178	**H**		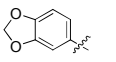	**29**	**90**	**1810**	**3294**	**30**	**458**
24	00010428	85239685	3233012	**Me**		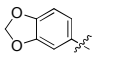	**36**	**22**	**692**	**8744**	**98**	**452**
25	00189310	99380783	46916176	**H**		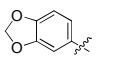	**70**	**173**	**584**	**435**	**17**	**83**
26	00185977	85239764	44223966	**H**	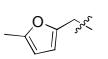	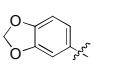	**15**	**39**	**651**	**> 10000**	**93**	**846**
27	00229611	99380786	46916179	**H**			**90**	**227**	**486**	**1320**	**76**	**313**

3.5 Cellular Activity

Cellular studies have not yet been run with these agents.

3.6 Profiling Assays

NCGC00188654/CID:44968231/ML167 has been run in Ambit's KinomeScan profile of 442 kinases. Language from the Ambit report describes the technology:

"KINOME*scan*™ is based on a competition binding assay that quantitatively measures the ability of a compound to compete with an immobilized, active-site directed ligand. The assay is performed by combining three components: DNA-tagged kinase; immobilized ligand; and a test compound. The ability of the test compound to compete with the immobilized ligand is measured via quantitative PCR of the DNA tag. The compound(s) were screened at the concentration(s) requested, and results for primary screen binding interactions are reported as '% Ctrl', where lower numbers indicate stronger hits in the matrix on the following page(s)."

Activities below a 10% threshold are currently being profiled for Kd values versus those targets. We further analyzed NCGC00188654/CID:44968231/ML167 for cell permeability in a commercially available Caco-2 assay. The Papp (A2B) was 32.0 with a percent recovery of 81.4% and the Papp (B2A) was 24.7 with a percent recovery of 81.2%. Atenolol (50% human absorption) and propranolol (90% human absorption) were used as a guide for ranking compounds in terms of permeability. Based on the values for these control compounds, the results for NCGC00188654/CID:44968231/ML167 suggest that this agent will be highly cell permeable.

4 Discussion

This report details a novel class of Clk inhibitors based upon a core 6-arylquinazolin-4-amine scaffold. Selected agents were screened versus Clk4 to gain an appreciation of this chemotype's SAR, and selected agents were found to inhibit this enzyme with potencies below 100nM. One early-stage analogue (**2**) was profiled against a panel of over 400 kinases and found to be remarkably selective for Clk1, Clk4 and Dyrk1A. The only other reported inhibitor of the Clk family [TG003 (**1**)] was also profiled and found to bind selectively to Clk1, Clk2, Clk4 and Dyrk1A. Analysis of the mechanism of action highly suggests that this chemotype inhibits Clk4 via competition with ATP binding. Molecular modeling also suggests that **2** and related agents inhibit the Clk isozymes through binding at the ATP binding domain. Further SAR evaluations have found newer agents with enhanced potency and selectivity profiles, including NCGC00188654/CID:44968231/ML167 (**7**), which we define as a probe of Clk4. These agents provide useful tools for the study of Clk1, Clk4 and Dyrk1A and their respective roles in pre-mRNA splicing.

4.1 Comparison to existing art and how the new probe is an improvement

NCGC00188654/CID:44968231/ML167 (**7**) is a more selective inhibitor of Clk4 when compared to NCGC00010037/CID:3232621)(**2**) and TG0003 (**1**).

4.2 Mechanism of Action Studies

We explored the binding modality of this chemotype by examining the inhibitory capacity of NCGC00010037/CID:3232621/SID:85239684 (**2**) in settings that varied both compound and substrate concentrations. The dose response curve of **2** in the presence of 3 different ATP concentrations demonstrated a loss in potency when ATP levels rose (Figure 6). Conversely, the percent activity of **1** in the presence of varying concentrations of the peptide substrate had no affect on the compound potency. This data highly suggests that NCGC00010037/CID:3232621 (**2**) is an ATP-competitive inhibitor of Clk4. Based upon the similarity of NCGC00188654/CID:44968231/ML167, it is expected that this agent is also an ATP-competitive inhibitor of Clk4.

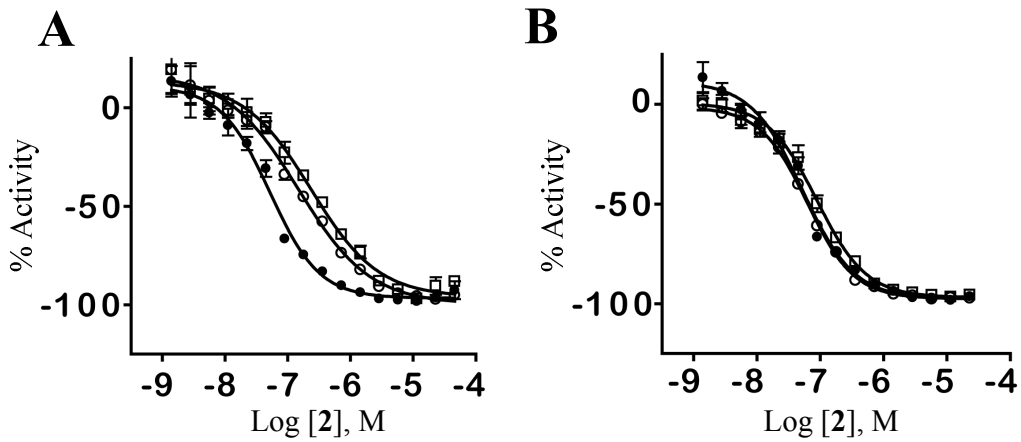

Figure 6. A. Inhibitory dose response of **2** in the presence of three different ATP concentrations [1μM (filled circles), 50μM (empty circles), 100μM (empty squares)]. B. Inhibitory dose response of **2** in the presence of three different peptide concentrations [50μM (filled circles), 100μM (empty circles), 200μM (empty squares)].

Following confirmation that this chemotype inhibits Clk4 via an ATP competitive mechanism, it was of interest to explore docking of **2** at a Clk kinase. As previously mentioned, quinazoline-based small molecules have precedence as kinase inhibitors. Among these reagents is the clinically approved drug erlotinib (Tarceva ®). Erlotinib is currently indicated for treatment of non-small cell lung and pancreatic cancer, and its actions are mediated through inhibition of the EGFR tyrosine kinase. In 2002, Stamos *et al* reported the structure of erlotinib bound to the ATP binding domain of EGFR (PDB code: 1M17). We theorized that the relationship of the 4-anilinoquinazoline structure of erlotinib to our newly discovered Clk family inhibitors may provide significant insight into the binding modality and mechanism of action for this class of compounds. There are no published X-ray structures of Clk4. There are structures of Clk1 (PDB code: 1Z57) and Clk3 (PDB code: 2EU9). Clk1 and Clk4 are highly homologous enzymes (>85% sequence identity), while Clk2 and Clk3 also share a high degree of sequence homology (>70% sequence identity). Based upon this, we utilized the X-ray structure of Clk1 as the template to derive a homology model of Clk4 using MOE molecular modeling software[18]. Molecular docking was performed on **2** within the ATP binding domain of Clk1 and Clk4 to achieve an optimal binding pose using FRED (Figure 7). In the crystal structure of erlotinib and EGFR, the N1 of the quinalozine heterocycle makes a critical H-bond to an amide NH of the hinge region of the ATP binding pocket. This interaction is mimicked within our docking analysis of **2** at Clk1 and Clk4. The thiophen-2-ylmethanamine moiety is oriented to fill an open

pocket formed by the gatekeeper Phe241 (Phe239 in Clk4), while the benzo[d][1,3]dioxole extends toward the solvent exposed face of the hinge region. While this model partially accounts for various aspects of the SAR found to date, more extensive exploration of this binding modality is required to fully understand the potency and remarkable selectivity associated with this chemotype.

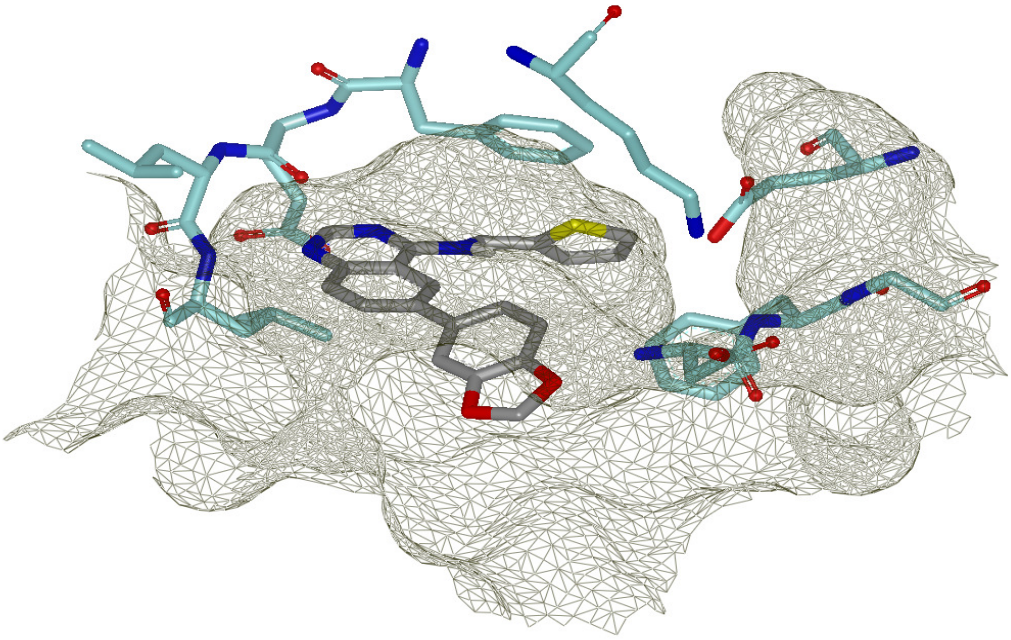

Figure 7. Docking model of **2** in the Clk1 catalytic cleft. The binding pocket is depicted by molecular surface in mesh grey and the hydrogen bonds are labeled as green dotted lines. This figure was prepared with the program VIDA (OpenEye Scientific Software).

4.3 Planned Future Studies

With good probes defined versus Clk4 (NCGC00188654/CID:44968231/ML167 (**7**)), Clk1/4 (NCGC00185963/CID:44223952), Dyrk1A (NCGC00229610/CID:469161787) and Dyrk1B (NCGC00185981/CID:44223970), we now intend to pursue collaborations to examine these agents in a variety of systems. Our first publication has already generated interested collaborators. For instance, a potential collaboration has been proposed surrounding the use of splicing modulators in the study of Spinal Muscular Atrophy (SMA). SMA is a severe congenital neurological disorder and a leading cause of mortality in infants and toddlers. There are approximately 50,000 patients in the US, EU and Japan. The disease is characterized by

progressive loss of motor neurons so patients lose the ability to walk, stand and move. Respiratory insufficiency is often fatal. The single known cause of SMA is mutations in SMN1, which encodes a protein involved in spliceosome assembly. Clk kinases regulate alternative splicing and so the modulation of these kinases pharmacologically may address functional deficiencies in SMA. Assistive technologies such as ventilators have improved the lives of SMA patients, but there are currently no approved therapeutic options for this condition.

Probe properties

Properties computed from Structure

Calculated Property	Probe Identity
	CID_44968231 (MLS002729079)
Molecular Weight [g/mol]	335.35658
Molecular Formula	C19H17N3O3
XLogP3-AA	2.7
H-Bond Donor	2
H-Bond Acceptor	6
Rotatable Bond Count	5
Tautomer Count	3
Exact Mass	335.126991
MonoIsotopic Mass	335.126991
Topological Polar Surface Area	84.3
Heavy Atom Count	25
Formal Charge	0
Isotope Atom Count	0
Defined Atom StereoCenter Count	0
Undefined Atom StereoCenter Count	0
Defined Bond StereoCenter Count	0
Undefined Bond StereoCenter Count	0
Covalently-Bonded Unit Count	1
Complexity	438

5 References

(1) Krämer, A. *Annu. Rev. Biochem.* **1996**, *65*, 367-409.

(2) Black, D. L. *Annu. Rev. Biochem.* **2003**, *72*, 291-336.

(3) Faustino, N. A.; Cooper, T. A. *Genes Dev.* **2003**, *17*, 419-437.

(4) Hanes, J.; von der Kammer, H.; Klaudiny, J.; Scheit, K. H. *J. Mol. Biol.* **1994**, *244*, 665-672.

(5) Nayler, O.; Stamm, S.; Ullrich, A. *Biochem. J.* **1997**, *326*, 693-700.

(6) Prasad, J.; Manley, J. L. *Mol. Cell. Biol.* **2003**, *23*, 4139-4149.

(7) Manley, J. L.; Tacke, R. *Genes Dev.* **1996**, *10*, 1569-1579.

(8) Zahler, A. M.; Lane, W. S.; Stolk, J. A.; Roth, M. B. *Genes Dev.* **1992**, *6*, 837-847.

(9) Hagiwara, M. *Biochemica et Biophysica Acta* **2005**, *1754*, 324-331.

(10) Mott, B. T.; Tanega, C.; Shen, M.; Maloney, D. J.; Shinn, P.; Leister, W.; Marugan, J. J.; Inglese, J.; Austin, C. P.; Misteli, T.; Auld, D. S.; Thomas, C. J. *Bioorg Med. Chem. Lett.* **2009**, *19*, 6700-6705.

(11) Hartmann, A. M.; Rujescu, D.; Giannakouros, T.; Nikolakaki, E.; Goedert, M.; Mandelkow, E.-M.; Gao, Q. S.; Andreadis, A.; Stamm, S. *Mol. Cell. Neuro.* **2001**, *18*, 80-90.

(12) Perni, R. B.; Bemis, J.; Nunes, J. J.; Szczepankiewicz, B. G. Inhibitors of the CDC2-like Kinases and Methods of Use Therof. WO 2009/085226 A2, 9 July 2009.

(13) Hekimi, S.; McBride, K.; Hihi, A. K.; Kianjcka, I.; Wang, Y.; Hayes, S. L.; Guimond, M.-P.; Sevigny, G.; Dumas, D.; Smith, J. New Quinoline Derivatives. 60/832937, 25 July 2006.

(14) Fan, F.; Wood, K. V. *Assay Drug Dev Technol* **2007,** 5, 127-36.

(15) Schroter, T.; Minond, D.; Weiser, A.; Dao, C.; Habel, J.; Spicer, T.; Chase, P.; Baillargeon, P.; Scampavia, L.; Schurer, S.; Chung, C.; Mader, C.; Southern, M.; Tsinoremas, N.; LoGrasso, P.; Hodder, P. *J Biomol Screen* **2008,** 13, 17-28.

(16) Singh, P.; Harden, B. J.; Lillywhite, B. J.; Broad, P. M. *Assay Drug Dev Technol* **2004,** 2, 161-9.

(17) Inglese, J.; Auld, D. S.; Jadhav, A.; Johnson, R. L.; Simeonov, A.; Yasgar, A.; Zheng, W.; Austin, C. P. Quantitative high-throughput screening: A titration-based approach that efficiently identifies biological activities in large chemical libraries. *Proc Natl Acad Sci U.S.A.* **2006**, *103*, 11473-8.

(18) MOE Molecular Operating EnVironment, Version 2008.10; Chemical Computing Group Inc.: Montreal, Canada, 2008.